

## Original Research Article

# Polyhydroxyalkanoate production during electroactive biofilm formation and stabilization in wetland microbial fuel cells for petroleum hydrocarbon bioconversion

Lanmei Zhao<sup>a</sup>, Mengxue Sun<sup>a</sup>, Can Lyu<sup>b</sup>, Long Meng<sup>a</sup>, Jian Liu<sup>b,c,\*</sup>, Bo Wang<sup>a,\*\*</sup>

<sup>a</sup> College of Chemical and Biological Engineering, Shandong University of Science and Technology, Qingdao, 266590, China

<sup>b</sup> Tobacco Research Institute of Chinese Academy of Agricultural Sciences, Qingdao, 266101, China

<sup>c</sup> Beijing Life Science Academy, Beijing, 102209, China



## ARTICLE INFO

## Keywords:

PHA production  
Biofilm  
Bioconversion  
Extracellular polymeric substances  
Functional microorganisms  
Network connections

## ABSTRACT

This study presented new insights into the sustainable conversion of total petroleum hydrocarbon (TPHC) into polyhydroxyalkanoates (PHAs) using wetland microbial fuel cells (WMFCs). The main innovations included the following two points: (1) The integration of bioelectricity generation with efficient PHA production further underscored the potential of electroactive biofilms as a sustainable platform for simultaneous TPHC biotransformation, bioelectricity recovery and PHA production. (2) The interactive dynamics of PHAs, metabolites, extracellular polymeric substances (EPS) and microorganisms during the formation and stabilization of electroactive biofilms provided novel insights into microbial strategies for carbon utilization. As the electroactive biofilm formed and stabilized, the current density enhanced significantly from 0 to 101 mA m<sup>-2</sup>, then stabilized, and finally dropped to 3.51 mA m<sup>-2</sup>. Similarly, the power density showed a trend of increasing in the initial stage, maintaining in the middle stage, and then descending in the later stage. The production of six types of PHAs was identified: poly(3-hydroxybutyrate) [P(3HB)], poly(3-hydroxyvalerate) [P(3HV)], poly(3-hydroxybutyrate-co-3-hydroxyvalerate) [P(3HB-co-3HV)], poly[(R)-3-hydroxybutyrate-co-(R)-3-hydroxyhexanoate] [P(3HB-co-3HHX)], poly(3-hydroxyhexadecanoate) [P(3HHD)] and poly(3-hydroxyoctadecanoate) [P(3HOD)], highlighting the metabolic flexibility of electroactive biofilms. The total PHA content was initially undetectable (days 0–4), gradually increased (days 4–28), rose rapidly (days 28–48), gradually increased and descended (days 48–68). The maximum PHA content of 0.664 g g<sup>-1</sup> DCW achieved highlighted the dual functionality of WMFCs in bioelectricity production and PHA biosynthesis, distinguishing it from conventional MFC applications. The TPHC biodegradation ratio demonstrated a gradual increase (days 0–28), with a more pronounced rise (days 28–48), and a gradual rise to 76.1 % (days 48–68). Throughout the process, the metabolite volatile fatty acids (VFAs) produced were primarily acetate, propionate, butyrate and valerate. The trend of VFA production from days 0–56 closely followed that of TPHC biodegradation. The trend of tyrosine/tryptophan proteins in EPS was aligned with that of biofilm thickness. The strong correlation between the increase in the biofilm thickness and the intensity and peak height of tyrosine/tryptophan proteins during the first 20 days suggested that these proteins were integral to the structural integrity of the biofilms, and from days 20–64, the minimal variation in their intensity and peak height indicated that the biofilms had reached a relatively stable state. The biofilms in turn provided a stable microbial substrate and energetic support for the subsequent efficient synthesis of PHA. During the early phase, the dual-function bacteria, such as *Pseudomonas*, *Bacillus*, *Acinetobacter* and *Desulfosarcina*, prioritized electron transfer and bioelectricity production using available carbon sources. As bioelectricity generation became less critical in the later phase, the bacteria shifted to intracellular PHA accumulation, transitioning from bioelectricity production to PHA biosynthesis. Finally, a comprehensive network connecting functional microorganisms with bioelectricity production, PHA content, TPHC biodegradation, VFA production and EPS peak height was established. Overall, these findings provided valuable insights into the dynamic interactions and

Peer review under the responsibility of Editorial Board of Synthetic and Systems Biotechnology.

\* Corresponding author. Tobacco Research Institute of Chinese Academy of Agricultural Sciences, Qingdao, 266101, China.

\*\* Corresponding author.

E-mail addresses: [liujian03@caas.cn](mailto:liujian03@caas.cn) (J. Liu), [wb@sdust.edu.cn](mailto:wb@sdust.edu.cn) (B. Wang).

<https://doi.org/10.1016/j.synbio.2025.01.008>

Received 25 October 2024; Received in revised form 30 December 2024; Accepted 22 January 2025

Available online 25 January 2025

2405-805X/© 2025 The Authors. Publishing services by Elsevier B.V. on behalf of KeAi Communications Co. Ltd. This is an open access article under the CC BY-NC-ND license (<http://creativecommons.org/licenses/by-nc-nd/4.0/>).

metabolic strategies of electroactive biofilms in WMFCs, highlighting their potential for the efficient bioconversion of PHCs into PHAs.

## 1. Introduction

Offshore wetlands served as a critical transitional area between land and sea, playing a vital role in bridging terrestrial and marine ecosystems. These wetlands ranked among the most productive ecosystems, offering important roles in preventing saltwater intrusion, purifying water, regulating climate and sustaining ecological functions [1,2]. However, the multi-factorial impacts of river runoff, wastes from municipalities and industries, maritime activities, and platform blowouts have exacerbated the accumulation of petroleum-based organic pollutants in offshore wetlands. The petroleum pollution not only risks destroying ecological functions, but also poses significant challenges for wetland remediation.

In response to this issue, bioelectrochemical systems (BES), particularly microbial fuel cells (MFCs), have gained increasing recognition as a promising method for remediating soil sediment polluted with petroleum hydrocarbons (PHCs) [3]. Notably, electroactive biofilms, which are central to the operation of MFCs systems, represent a unique microbial consortium with high metabolic activity, robust cell viability, and the ability to utilize complex organic pollutants, including PHCs [4]. Beyond their role in PHC biotransformation, the electroactive biofilms with high microbial activity and productivity coupled with the abundant carbon sources from PHC-contaminated wetlands are most likely to offer great advantages and potential to redirect carbon fluxes toward the synthesis of valuable bioproducts, such as PHAs.

The synthesized PHAs by microorganisms have applications in a variety of sectors, including industry, pharmaceuticals and biomedicine, due to their biocompatibility and elastomeric characteristics [5]. The use of hydrocarbons-based substrates for PHA production garnered significant interest because of the reduced cost of substrates, friendly environmental treatment and low CO<sub>2</sub> emissions. Various hydrocarbons were successfully utilized as carbon sources for PHA production by different microorganisms, achieving diverse yields. For example, spent engine oil, waste transformer oil, diesel, kerosene, crude oil, biphenyl, *n*-octane, *n*-decane and *n*-dodecane were used to synthesize PHAs such as P(3HB), P(3HB-co-3HV), Poly(3-hydroxybutyrate-co-3-hydroxyoctanoate), Poly(3-hydroxyheptanoate), P(3HHO), P(3HOD) and other mcl-PHAs, with production yields ranging from 7 % to 60 % depending on the substrates and microbial strains [6–11]. These findings collectively underscored the versatility and effectiveness of PHC-based substrates in the production of PHAs by the isolated bacteria. Despite the demonstrated versatility of isolated bacteria in utilizing PHCs as substrates for PHA production, the potential for PHA synthesis based on electroactive biofilms during the electro-conversion of PHCs in WMFCs remains largely unexplored. This issue deserves further in-depth exploration.

EPS, the pivotal constituents of electroactive biofilms, assumed a key role in biofilm formation and stabilization [4]. The previous researchers have done some explorations on the effect of EPS on PHA generation. EPS production was demonstrated to have a negative impact on PHA yield, given that both processes relied on carbon substrates and energy [12]. Despite this trade-off, EPS provided critical protective functions, shielding microbial communities from the inhibitory effects of toxic substrates. The stable performance of EPS-producing sludge was shown to support consistent biomass levels, which were essential for sustained PHA production [13]. Additionally, EPS-producing bacteria in sludge were found to facilitate the development of PHA-producing bacteria [14]. Importantly, the previous research demonstrated a distinct mathematical relationship between PHA and EPS, indicating that carbon flow tended to favor PHA synthesis over EPS production in carbon-rich environments [15]. The extant literature on the effect of EPS on PHA

synthesis has yielded equivocal results. Therefore, these conflicting results underscored the need for further investigation to take EPS into account in the exploration of PHA production based on electroactive biofilms in WMFCs. In addition to this, the key metabolites during PHC biotransformation, such as VFAs, which can also serve as advantageous substrates for PHA production [16], should also be taken into account.

Given these insights, PHA production based on electroactive biofilms in WMFCs for PHC bioconversion remains poorly understood. To address this knowledge gap, this study aims to investigate PHA production during electroactive biofilm formation and stabilization in WMFCs for PHC bioconversion, focusing on PHA content, metabolite production, EPS generation, microbial community function and their network connections. By exploring the dual role of electroactive biofilms in PHC-polluted wetland remediation and bioproduct synthesis, this research seeks to advance microbial resource utilization and provide sustainable solutions for wetland environments.

## 2. Materials and methods

### 2.1. WMFC biosystem construction

The WMFC biosystem used in this study was presented in Fig. 1. A cylindrical plexiglass container with a height of 40 cm and a diameter of 30 cm was employed as the reaction chamber. Each chamber was filled with 4 kg of uncontaminated wetland soil (sludge-water mixture) and a cleaned reed was planted inside, while the PHCs from Shengli oilfield (Dongying, China) were added at a concentration of 5 g/kg to simulate a PHC-polluted wetland environment. The PHC level was based on measurements taken from certain reed rhizospheres in the Yellow River Delta (Dongying, China), where the concentration could achieve approximately 5 g/kg. The PHCs were consisted of 89.2 % aliphatics

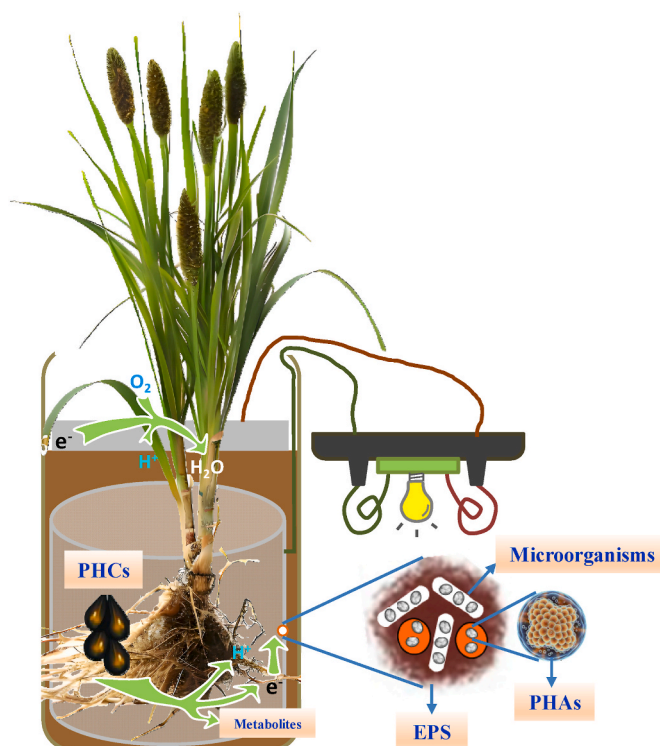


Fig. 1. The WMFC biosystem used in this study.

(with C<sub>6</sub>–C<sub>18</sub> alkanes accounting for the largest proportion), 10.4 % aromatics and a small amount of other organic compounds. To maintain a stable temperature, heating tape was wrapped around the reaction chamber, which was set to 30 °C. Carbon fiber brushes were employed as electrodes, with a cylindrical anode, measuring 0.1256 m<sup>2</sup>, positioned vertically around the outer edge of the reed rhizosphere. Meanwhile, the cathode was positioned horizontally on the wet soil surface, which was exposed to the air. An external load was provided by connecting a 1000 Ω resistor between the cathode and anode. Three sets of parallel experiments were provided, each with 17 of the same WMFC biosystems, and the entire experiment was conducted over 68 days under a closed circuit. An observation was made regarding the formation and stabilization of anode biofilms. The biofilm samples were taken at that time, with the intention of conducting subsequent tests and analyses. To prevent subsequent sampling from influencing the established biosystems, the biofilm samples were collected once from each WMFC biosystem throughout the course of the experiment. By the end of the experiment, 17 biofilm samples were obtained in parallel triplicate.

## 2.2. Testing and analysis methods

### 2.2.1. Bioelectricity production performance

The current (I) and output voltage (U) of WMFCs were continuously recorded during anode biofilm formation and stabilization. The I was measured continuously with a precision multimeter that was integrated into a data acquisition system, whereas the U was recorded using a multichannel voltage recorder. The current density was obtained by formula I/A. The power density was determined by means of the following equation:  $P = UI/A$ , where A denoted the surface area of the anode.

### 2.2.2. PHA extraction and measurement

The biofilm samples intended for testing were subjected to a centrifugal process at an angular velocity of  $11,200 \times g$  for a duration of 10 min. Thereafter, the samples were suspended in deionized water and underwent three wash cycles. The resultant washed biofilms were collected and subsequently freeze-dried. The freeze-dried samples were then subjected to gravimetric analysis to determine the dry cell weight (DCW). 3.5 g DCW was added to a solution comprising 75 mL of chloroform and 75 mL (30 % v/v) of sodium hypochlorite. The mixed solution was stirred for a period of 2.5 h at a temperature of 30 °C. The upper white layer was removed, and the remaining portion was subjected to centrifugation at 8000 rpm for a period of 15 min, with the objective of collecting the chloroform phase, in which the PHA was present. A quantity of 2 mL of chloroform phase was added to an esterification tube, along with 2 mL of an esterification solution comprising a methanol solution containing 1 g L<sup>-1</sup> benzoic acid and 3 % (v/v) concentrated sulfuric acid. The tube was then covered and sealed tightly, and the reaction was esterified at 100 °C for 4 h. Upon cooling to room temperature, 1 mL of deionized water was added, and the contents of the tube were fully shaken and mixed well. The mixture was then allowed to settle. Following the complete separation of the chloroform phase from the aqueous phase, the chloroform phase was taken and tested by gas chromatography-mass spectrometry (GC-MS) (6890-5973 N, Agilent, USA) [17]. An HP-5 (30 m × 0.32 mm × 0.25 μm) column was utilized, with the column temperature increased from 50 °C to 260 °C in a 10 °C gradient. The ionization mode was electron impact (EI), and the temperature of ion source was 230 °C. The carrier gas was helium at a flow rate of 1.0 mL min<sup>-1</sup>. The temperature of the injection port was 290 °C, and the injection volume was 1 μL.

### 2.2.3. TPHC degradation and metabolite VFA determination

For TPHC degradation determination, TPHC concentration was determined by UV–visible spectrophotometry at 225 nm [18]. Petroleum ether was used to extract TPHCs from sludge-water mixture, and this procedure was conducted on three occasions to ensure the accuracy

of the results. For metabolite VFA determination, high performance liquid chromatography (HPLC) (Agilent 1260, USA) was used [4]. A volume of 10 μL of the water phase present in the sludge-water mixture, following the processes of centrifugation and filtration, was employed in the execution of this HPLC test.

### 2.2.4. EPS extraction and determination

EPS from biofilms were extracted by using ultrasonic extraction method [19], and the methodology employed for the extraction procedure was delineated in exhaustive detail by Yu et al. Fluorescence analysis (three-dimensional excitation-emission matrix, 3D-EEM) was employed to detect the type and fluorescence intensity of EPS.

### 2.2.5. Microbial community measurement and analysis

The high-throughput sequencing of biofilm samples was conducted at Major Bio-group (Shanghai). Following the extraction of total DNA, its quality was assessed through the utilization of 1 % agarose gel electrophoresis. Barcoded primers specific to the selected sequencing region were synthesized. Subsequently, PCR amplification was conducted through TransGen AP221-02 TransStart® FastPfu DNA Polymerase. The obtained PCR products were purified by excising the target bands with the AxyPrep DNA Gel Recovery Kit (AXYGEN) and subsequently eluted in Tris-HCl buffer. Following this, verification was conducted through 2 % agarose gel electrophoresis. The library was constructed and sequenced on the Illumina PE300 platform. The resulting raw sequencing data underwent quality control, sequence assembly, OTU clustering and data analysis, resulting in outputs such as species annotation, composition analysis, species diversity comparison and sample-level comparative assessments.

### 2.2.6. Network connections establishment

The network connection of functional microorganisms with bioelectricity, PHAs, TPHCs, VFAs and EPS during electroactive biofilm formation and stabilization was analyzed by using Pearson correlation ( $P < 0.05$ ) and presented as heatmap.

## 3. Results and discussion

### 3.1. Bioelectricity generation performance and PHA content during electroactive biofilm formation and stabilization in WMFCs

#### 3.1.1. Electroactive biofilm formation and stabilization in WMFCs

The biofilm thickness exhibited a notable rise with the duration of WMFC operation, with the initial thickness of 0 μm increasing significantly over time (Fig. 2a). During the initial 20 days period, the thickness exhibited a particularly rapid rise, increasing from 0 μm to approximately 678 μm. The rising trend in biofilm thickness indicated that microorganisms quickly colonized the anode surface, consistent with typical electroactive biofilm growth dynamics. This was also a critical phase for WMFC performance as the biofilms served as the primary site for microbial activity, including TPHC degradation and electron transfer to the anode [4]. Following a period of approximately 20 days, the biofilm thickness demonstrated minimal change and reached a point of stabilization. By the conclusion of the experiment (68 days), the thickness remained within the range of 678–691 μm. The stabilization of biofilm thickness after day 20 indicated that the biofilm reached a mature and stable state, where microbial growth and detachment were in equilibrium. This stabilization was essential for sustained bioelectricity generation, as a well-established biofilm ensured efficient electron transfer and a stable electrochemical environment [20]. The changing trend in biofilm thickness indicated that microorganisms gradually formed and accumulated on the anode surface with the extension of operational time, thereby forming a stable biofilm structure. This process is of great importance for the enhancement of WMFC performance, given that the microorganisms present within the biofilm are the primary contributors responsible for the degradation of TPHCs

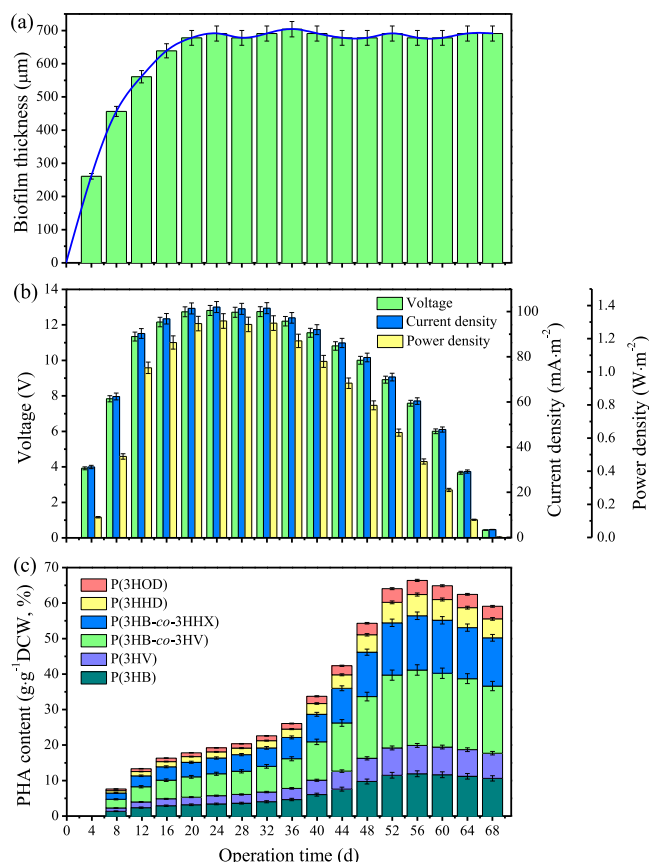


**Fig. 2.** (a) Biofilm thickness, (b) output voltage, current density, power density, and (c) PHA content during electroactive biofilm formation and stabilization in WMFCs.

and the generation of bioenergy.

### 3.1.2. Bioelectricity generation performance during electroactive biofilm formation and stabilization

The output voltage, current density and power density during electroactive biofilm formation and stabilization were showed in Fig. 2b. The output voltage started at 0 V and exhibited a notable increase with the thickening of biofilms (days 0–20), reaching a peak value (12.7 V) at the time of biofilm stabilization (day 20). The value remained stable (12.7–12.8 V) during the initial phase of biofilm stabilization (days 20–32). At the subsequent stage of biofilm stabilization (days 32–68), the output voltage displayed a gradual decline, achieving a value of 0.44 V. A similar trend was observed in the current density, which enhanced significantly from 0 to 101 mA m<sup>-2</sup>, then stabilized, and finally dropped to 3.51 mA m<sup>-2</sup>. The power density also showed a trend of increasing in the initial stage, maintaining in the middle stage, and then descending in the later stage. In contrast to output voltage and current density variations, the rising and falling periods of power density changed more sharply. The changing trends in output voltage, current density and power density (Fig. 2b) closely followed the biofilm formation process, further emphasizing the critical role of biofilm development in WMFCs. The sharp rise in output voltage, current density and power density during the initial 20 days corresponded to the phase of rapid biofilm growth, where microbial colonization and activity were at their peak on day 20. During the early stabilization phase of biofilms (days 20–32), the stable performance of bioelectricity production indicated that the biofilms were functioning efficiently, with high microbial activity and effective electron transfer. However, after about 12 days of stabilization, the performance of electricity production

gradually declined with the continuous consumption of substrate, as evidenced by a decrease in output voltage, current density and power density. The gradual decline in bioelectricity generation after day 32 could be attributed to substrate consumption. As the available TPHCs and other organic substrates were consumed, microbial activity likely decreased, and consequently led to a reduction in electron transfer, which was manifested by the drop in output voltage, current density and power density. This decline in bioelectricity generation performance highlighted the importance of substrate availability for sustained bioelectricity generation.

Microbial electrochemical systems (MESs), including Soil MFCs (SMFCs), have been demonstrated to be promising for treating petroleum hydrocarbons (PHCs). For instance, Chen et al. achieved a remediation efficiency of 74 % for soil contaminated with 7258 mg/kg PHCs using a microbial electrochemical system with carbon felt and titanium wiring as electrodes, stimulated with iron minerals over 148 days, producing a maximum current density of 164 mA/m<sup>2</sup> [21]. Similarly, Wang et al. reported a remediation efficiency of 76 % for soil contaminated with 24,085 mg/kg crude oil in a bottle-type dual-chamber MFC with a carbon fiber brush anode and titanium wire mesh cathode, yielding a maximum current density of 569 mA/cm<sup>2</sup> over 140 days [22]. In another study, Zhang et al. used a cylindrical SMFC with a carbon cloth anode and activated carbon cathode to remediate soil containing 83,060 mg/kg PHCs, achieving a remediation efficiency of 52 % and a power density of 132 mW/m<sup>2</sup> over 182 days [23]. For phenanthrene-contaminated soils, Zhao et al. utilized single-chamber plant-MFCs with graphite felt electrodes and surfactant addition, achieving a remediation efficiency of 45 % and a maximum voltage of 185 mV in 35 days, while Liang et al. reached a remediation efficiency of 78.1 % in 110 days using an SMFC with a carbon nanomaterial-modified graphite felt anode [24,25]. Yu et al. demonstrated a remediation efficiency of 59.1 % for 11,632 mg/kg PHCs using an SMFC with a graphite felt cathode and activated carbon fiber felt anode, with a power density of 24.0 mW/m<sup>2</sup> over 115 days [26]. Additionally, Zhao et al. and Zhang et al. achieved remediation efficiencies of 22.8 % and 56 %, respectively, for PHC-contaminated soils using graphite fiber brush and carbon cloth electrodes in cylindrical SMFCs, with bioelectricity outputs of 0.4 mA and 57 mV, respectively [27,28]. Compared to previous studies, this research demonstrated significant advantages in both bioelectricity generation and remediation efficiency. The output voltage (12.7 V), current density (101 mA m<sup>-2</sup>) and power density (1.29 W m<sup>-2</sup>) achieved during the biofilm stabilization phase surpassed many reported values, highlighting the superior performance of the WMFC systems. Additionally, the study explored in detail the dynamics of bioelectricity generation during the formation of electroactive biofilms, providing valuable insights into the dynamic correlation between bioelectricity production and biofilm development. Furthermore, the maximum PHA content of 0.664 g g<sup>-1</sup> DCW achieved in this study (as reported in Section 3.1.3) underscored the dual functionality of WMFCs in both PHC biotransformation and bioproduct synthesis, setting it apart from conventional SMFC applications.

### 3.1.3. PHA content during electroactive biofilm formation and stabilization

The various types of produced PHA included P(3HB), P(3HV), P(3HB-co-3HV), P(3HB-co-3HHX), P(3HHD) and P(3HOD) (Fig. 2c). The undetectable PHA content from days 0–4 was expected, as the biofilm had not yet fully formed, and microbial activity was likely insufficient to induce significant PHA biosynthesis. The gradual increase in total PHA content from days 4–28, followed by a rapid rise from days 28–48, could be attributed to the progressive establishment of stable electroactive biofilms. During the early stage of biofilm formation (days 0–20), microbial colonization and growth were still in progress, resulting in relatively low PHA production. This was consistent with the observation that the biofilm thickness and bioelectricity generation were also in their initial growth phases during this period (Fig. 2a and b). The rapid rise in PHA content from days 28–48, peaking at day 56 with a maximum value



of  $0.664 \text{ g g}^{-1}$  DCW, suggested that the microbial community had reached a high level of metabolic activity, likely driven by the availability of TPHCs as carbon sources. This phase of rapid PHA accumulation could be linked to the abundance of degradable organic substrates, which provided the necessary precursors for PHA biosynthesis.

P(3HB-co-3HV) and P(3HB-co-3HHX) accounted for the largest yields of approximately 32 % and 23 % of the total PHA content, respectively. This was followed by P(3HB) and P(3HV), representing approximately 18 % and 12 %, and finally P(3HHD) and P(3HOD), representing approximately 9 % and 6 %, respectively. The diversity in PHA compositions highlighted the metabolic flexibility of electroactive biofilms and its ability to adapt to the available carbon sources, which was crucial for effective TPHC bioconversion. The predominance of P(3HB-co-3HV) and P(3HB-co-3HHX) suggested that the microbial community favored the synthesis of copolymers. These copolymers are often produced when a diverse range of carbon substrates is available, as is likely the case in the WMFCs due to the presence of complex hydrocarbons from TPHC contamination. The relationship between bioelectricity generation and PHA production was particularly noteworthy. During the stable period of bioelectricity generation (days 20–32), PHA content went up steadily and then rapidly, suggesting that the microorganisms within the biofilms were not only contributing to bioelectricity generation but also actively diverting carbon substrates toward PHA biosynthesis. During this period, the biofilms reached a stable thickness, and bioelectricity generation was at its peak, suggesting that the microbial populations had shifted toward a more efficient state of electron transfer and substrate utilization. During the period of decline in bioelectricity generation (days 32–68), PHA content exhibited an initial rapid increase, followed by a period of steady growth and subsequently a gradual decline. The initial rapid increase in PHA content during the decline in bioelectricity generation reflected that microorganisms were redirecting the carbon derived from TPHC biodegradation toward PHA biosynthesis. This shift was likely due to the stabilization of the electroactive biofilms, where the microbial community had already established sufficient biofilm structure and was no longer prioritizing energy generation through bioelectricity. Instead, the carbon substrates were increasingly funneled into PHA production, a typical microbial strategy for storing excess carbon under nutrient-limited or stress conditions [15,29].

Several explorations have been made to synthesize PHAs from single or mixed PHCs. For instance, when spent engine oil was utilized as a carbon source, *Achromobacter*, *Alcaligenes* and *Ochrobactrum* successfully synthesized P(3HB), Poly(3-hydroxybutyrate-co-3-hydroxyoctanoate) and Poly(3-hydroxyheptanoate), with production yields varying between 20 % and 46 % [9]. In the case of waste transformer oil as the substrate, *Acinetobacter*, *Bacillus*, *Proteus*, and *Serratia* were able to intracellularly produce P(3HHD) and P(3HOD), achieving yields ranging from 7 % to 33.1 % [6]. When diesel, kerosene, crude oil and oily bilge water were employed as substrates, *Ochrobactrum intermedium* synthesized P(3HB) with yields between 30 % and 41 % [8]. Additionally, for the substrate biphenyl, *Achromobacter denitrificans* A41 produced P(3HB-co-3HV) at yields ranging from 10 % to 48 % [11]. When phenanthrene, pyrene, and fluoranthene were used, *Pseudomonas aeruginosa*, *Pseudomonas putida* and *Cupriavidus necator* were capable of producing mcl-PHAs, with yields ranging from 40 % to 50 % [10]. Furthermore, using *n*-octane, *n*-decane and *n*-dodecane as substrates, *Pseudomonas resinovorans* ATCC 12498 achieved a maximum yield of 60 % in the production of mcl-PHAs [7]. When single PHCs, e.g., octadecane, *n*-dodecane, *n*-decane and octane, were used as carbon sources, the types of PHA produced mainly included P(3HB), P(3HV), P(3HB-co-3HV), etc., consisting predominantly of scl- and mcl-PHAs, with the highest yield of  $60 \text{ g g}^{-1}$  DCW [30,31]. When mixed PHCs such as spent engine oil, waste transformer oil, oily bilge water, kerosene and crude oil were served as carbon sources, the types of PHA produced included P(3HB), P(3HV), P(3HHD), P(3HOD), etc., comprising scl-

mcl- and lcl-PHAs, with the maximum yield of  $46 \text{ g g}^{-1}$  DCW [30]. Compared to previous studies, this research demonstrated significant advantages in PHA production and diversity, achieving the highest PHA content of  $0.664 \text{ g g}^{-1}$  DCW, surpassing the maximum yield ( $60 \text{ g g}^{-1}$  DCW) reported from previous studies. The WMFC systems enabled the production of a wide range of PHAs, highlighting the metabolic flexibility of electroactive biofilms. Unlike earlier studies that relied on specific microbial strains or single substrates, this study utilized TPHCs, demonstrating superior adaptability and scalability for real pollutant applications. Furthermore, the dynamic relationship between bioelectricity generation and PHA synthesis provided novel insights into microbial strategies for carbon utilization.

### 3.2. TPHC biodegradation and VFA production during electroactive biofilm formation and stabilization in WMFCs

The TPHC biodegradation ratio demonstrated a gradual increase from days 0–28, with a more pronounced rise from days 28–48, and a gradual rise to 76.1 % from days 48–68 (Fig. 3), suggested that the microbial community within the biofilm became progressively more efficient at degrading TPHCs as the biofilm matured. This process was essential for the WMFC system, as TPHC biodegradation not only contributed to the remediation of contaminated environments but also provided the necessary substrates for microbial metabolism, which in turn drove bioelectricity generation and PHA production [16,20]. During the period of biofilm formation (days 0–20), the trend of TPHC biodegradation ratio was found to align with that of bioelectricity generation performance (Fig. 2b). This indicated that, at this early stage, the primary metabolic focus of the microbial community was on the conversion of TPHCs into electrons for bioelectricity production. As the biofilm matured and entered the stabilization phase (days 20–56), the changing trend of TPHC biodegradation ratio became more closely consistent with PHA content (Fig. 2c). This shift indicated that, during biofilm stabilization, the microbial community began diverting more of the carbon derived from TPHC biodegradation toward PHA biosynthesis rather than bioelectricity generation. This metabolic shift reflected the fact that, once the biofilms reached a stable state, the microorganisms had sufficient energy to support both electron transfer and intracellular PHA storage. The rapid increase in PHA content from days 28–48 further supported this, as the microbial community likely utilized the intermediate metabolites as carbon sources for PHA accumulation during this period of high metabolic activity. After day 56, the growth of TPHC biodegradation ratio slowed, which coincided with a decline in PHA content (Fig. 2c). This reflected that the continuous consumption of substrates became a limiting factor for PHA biosynthesis at this stage. The gradual depletion of TPHCs likely reduced the carbon flux available for both bioenergy production and PHA biosynthesis, leading to the observed decrease in PHA content. This highlighted the importance of substrate availability for sustaining both TPHC bioconversion and PHA

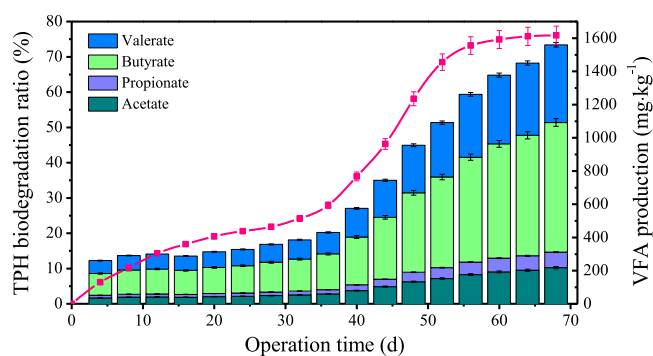


Fig. 3. TPHC biodegradation ratio and VFA production during electroactive biofilm formation and stabilization in WMFCs.

production in WMFC systems. Compared to previous studies (as reported in Section 3.1.2), this research demonstrated significant advancements in TPHC biodegradation, achieving a high biodegradation ratio of 76.1 % alongside the production of bioelectricity and PHAs, which highlighted the multifunctionality of WMFC systems. Unlike prior studies that focused primarily on bioremediation or bioelectricity generation, this study revealed a dynamic metabolic shift in the microbial community, effectively balancing TPHC degradation, bioelectricity generation and PHA biosynthesis. Additionally, the detailed analysis of TPHC biodegradation during the formation of electroactive biofilms and the substrate utilization by PHA biosynthesis or bioelectricity generation provided novel insights into optimizing microbial electrochemical systems for sustained performance.

The metabolite VFAs produced throughout the process were primarily acetate, propionate, butyrate and valerate (Fig. 3). VFAs were key intermediates in TPHC bioconversion and served as important substrates for both microbial growth and PHA biosynthesis [16]. Butyrate and valerate accounted for the largest proportion of the total VFAs (approximately 50 % and 30 %, respectively), which were the predominant components in VFAs. This was followed by acetate, which represented approximately 14 % of the total VFAs. The predominance of butyrate and valerate reflected that these VFAs were the primary intermediates produced during TPHC bioconversion. This also indicated that the microbial community was actively breaking down complex TPHCs into simpler, short-chain fatty acids, which could then be utilized for further metabolic processes [17]. The changing trend of total VFA production from days 0–56 closely followed the trend in TPHC biodegradation ratio, indicating that VFA production was directly linked to the microbial breakdown of TPHCs. As the microorganisms degraded TPHCs, they produced VFAs as intermediates, which reflected the enhanced microbial activity and substrate utilization during this period. This was consistent with the observed increase in both bioelectricity generation and PHA content, as the produced VFAs served as key intermediates fueling both processes. Interestingly, in contrast to TPHC biodegradation ratio, the total VFA production rose significantly after day 56, while PHA production descended at this stage. This indirectly suggested that the reduced capacity of PHA biosynthesis may lead to the accumulation of VFAs (Figs. 2 and 3), which served as the main substrate required for PHA biosynthesis [16,17].

### 3.3. EPS composition and strength during electroactive biofilm formation and stabilization in WMFCs

EPS played a critical role in the formation, stabilization, and functionality of electroactive biofilms. Three-time nodes, days 0, 20, and 32, when the bioelectricity generation performance changed (Fig. 2b), and six-time nodes, days 0, 4, 28, 48, and 56, when the PHA content changed, and day 64, which is the middle of the declining branch of PHA content (Fig. 2c), for a total of eight-time nodes, were selected to compare the composition and strength of EPS in electroactive biofilms under these eight-time nodes. EPS composition and strength during electroactive biofilm formation and stabilization were depicted in Fig. 4. The regions A, B, C, D and E represented tyrosine/tryptophan proteins, polysaccharides, polycarboxylate-type humic acids, polyaromatic-type humic acids and fulvic acids, respectively. The tyrosine/tryptophan proteins exhibited the highest fluorescence strength and the most notable alterations among the five components. In contrast, the remaining four components displayed markedly lower fluorescence strength and insignificant changes. This suggested that tyrosine/tryptophan proteins played a particularly important role in the structural and functional dynamics of electroactive biofilms. From days 0–20, there was a notable increase in the intensity and peak height of tyrosine/tryptophan proteins, indicating a robust positive trajectory. This period coincided with the rapid increase in biofilm thickness (Fig. 2a) and the sharp rise in bioelectricity generation (Fig. 2b), suggesting that tyrosine/tryptophan proteins contributed significantly to both biofilm development and electrochemical activity. Their enhancement during the early biofilm formation phase reflected the active synthesis of proteins required for microbial attachment to the anode surface and the establishment of stable biofilm matrix [4]. These proteins also played a role in facilitating electron transfer between microorganisms and the electrode, given that aromatic amino acids could participate in redox reactions and electron shuttling [20].

The strong correlation between the increase in tyrosine/tryptophan proteins and biofilm thickness during the first 20 days suggested that these proteins were integral to the structural integrity of the biofilms. As the biofilm thickened, these proteins contributed to the formation of robust matrix that supported microbial growth and enhanced the biofilm's ability to conduct electrons, thereby improving the overall bioelectricity generation performance. From days 20–64, the intensity and peak height of tyrosine/tryptophan proteins exhibited minimal variation, indicating that the biofilm had reached a relatively stable

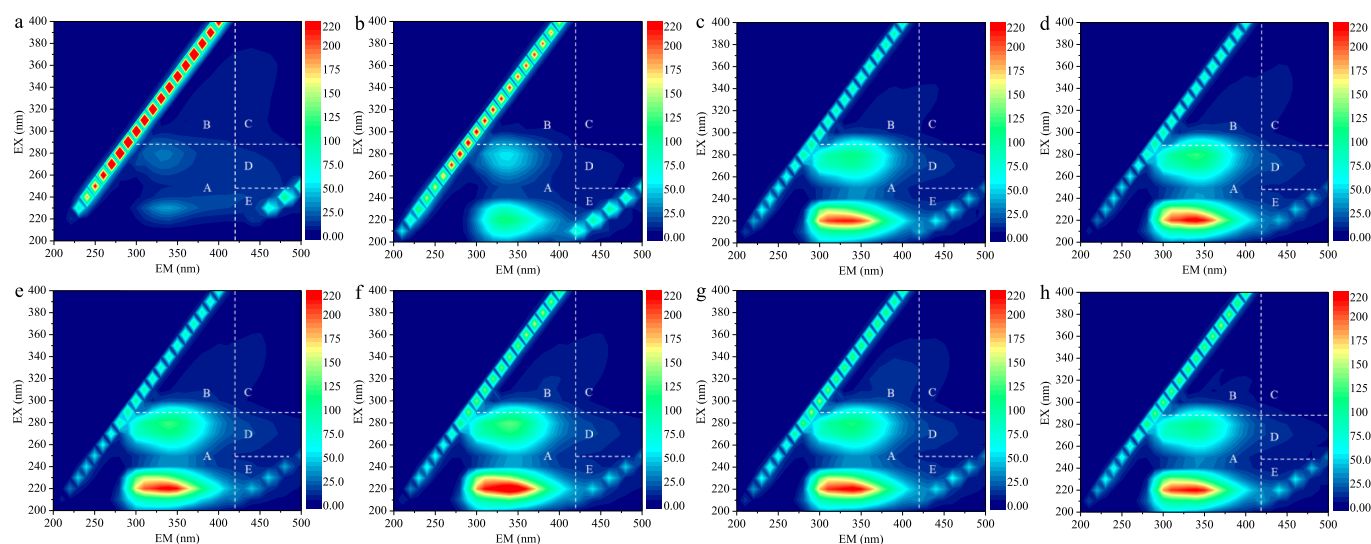


**Fig. 4.** EPS composition and strength during electroactive biofilm formation and stabilization in WMFCs (a-h denoted the electroactive biofilm samples on days 0, 4, 20, 28, 32, 48, 56 and 64, respectively).

state in terms of EPS compositions. This stabilization phase aligned with the period of stable biofilm thickness (Fig. 2a) and bioelectricity generation (Fig. 2b), suggesting that the biofilm had matured and reached an equilibrium where microbial growth, detachment and EPS production were balanced. The stabilization of tyrosine/tryptophan proteins during this period also reflected that once the biofilm matrix was fully established, the need for further EPS production diminished. The biofilms reached a point where its structure was sufficiently robust to support the continued electron transfer and the microbial activity involving PHA synthesis without the need for additional EPS synthesis.

Previous studies have preliminarily explored the effect of EPS on PHA generation, revealing a complex interplay between the two processes. It was demonstrated that EPS production could negatively impact PHA yields, as both pathways competed for the same carbon substrates and energy resources [12]. Despite this trade-off, EPS played a critical role in protecting microbial communities by mitigating the inhibitory effects of toxic or harsh environmental conditions, such as exposure to PHCs or other pollutants. This protective function ensured the stability and resilience of microbial biomass, which was essential for maintaining consistent PHA production over time [13]. Furthermore, EPS-producing bacteria were shown to facilitate the establishment and growth of PHA-producing microorganisms within complex microbial consortia, creating a supportive environment for efficient PHA production [14]. Notably, prior research suggested that in carbon-rich environments, microbial communities tended to prioritize carbon flux toward PHA synthesis rather than EPS production [15]. However, the available literature presented mixed findings regarding the precise effects of EPS on PHA biosynthesis, with some studies emphasizing the competitive nature of the two processes, while others highlighted their complementary roles in microbial community dynamics. Compared to previous studies, this research provided a deeper understanding of the dynamic role of EPS, particularly tyrosine/tryptophan proteins, in the formation, stabilization and functionality of electroactive biofilms. By linking EPS composition and strength with biofilm development, bioelectricity generation and PHA production across eight-time nodes, this study offered a comprehensive analysis of the interplay between these processes. Unlike prior research that mainly focused on the competitive

relationship between EPS and PHA, this study highlighted their complementary roles, demonstrating that EPS not only supported biofilm stability and electron transfer but also facilitated conditions for efficient PHA synthesis. The identification of tyrosine/tryptophan proteins as key contributors to biofilm integrity and electrochemical activity provided novel insights into optimizing biofilm performance.

#### 3.4. Microbial community function during electroactive biofilm formation and stabilization in WMFCs

The heatmap of microbial community compositions (Fig. 5) revealed significant shifts in the relative abundance of key functional bacteria over time, which were closely aligned with the observed trends in bioelectricity generation (Fig. 2b) and PHA production (Fig. 2c). These results highlighted the complex interplay between electrochemically active bacteria (EAB) and PHA-synthesizing bacteria (PHASB) during the formation and stabilization of electroactive biofilms, as well as the functional versatility of certain bacteria that contributed to both processes.

*Desulfuromonas*, *Bacillus*, *Brevundimonas*, *Clostridium*, *Acidibacter*, *Geobacter*, *Flavobacterium*, *Shewanella*, *Acinetobacter*, *Desulfosarcina*, *Pseudomonas* and *Pelotomaculum*, as EAB, possessed the ability to transfer electrons and generate bioelectricity during PHC biotransformation. Their mechanism of bioelectricity generation was demonstrated through the effective transfer of electrons, either directly or indirectly, facilitated by external electron mediators, self-synthesized C-type cytochromes or their conductive pili [20]. In addition, *Pseudomonas*, *Cupriavidus*, *Bacillus*, *Alcanivorax*, *Rhodococcus*, *Acinetobacter*, *Alcaligenes*, *Ochrobactrum*, *Halomonas*, *Enterobacter*, *Paracoccus*, *Thauera* and *Desulfosarcina*, as PHASB, were capable of synthesizing scl-, mcl- or lcl-PHAs through ingesting PHC components such as spent engine oil, waste transformer oil, crude oil, aromatic hydrocarbons or alkanes [6, 10,30,31]. *Pseudomonas* had the capability to produce mcl-PHAs, and the presence of 3-hydroxydecanoate and 3-hydroxyoctanoate in the cells confirmed the feasibility of synthesizing intracellular PHAs using *Pseudomonas putida* KT2440 [32]. The specific genes of *Pseudomonas aeruginosa* could be co-expressed with PHA synthase to elevate the

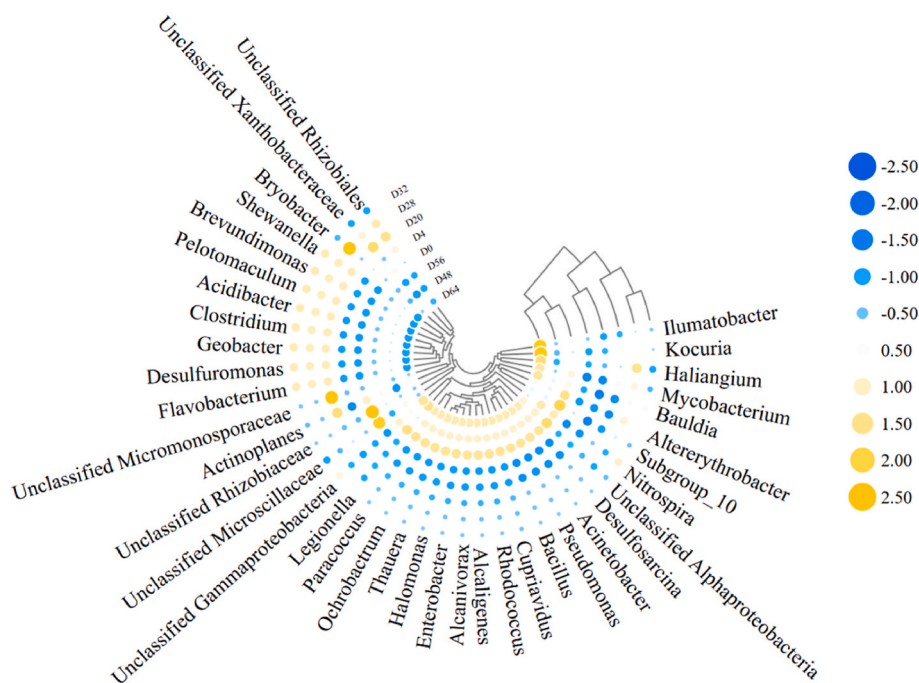


Fig. 5. Microbial community heatmap of electroactive biofilms (D0, D4, D20, D28, D32, D48, D56 and D64 denoted the electroactive biofilm samples on days 0, 4, 20, 28, 32, 48, 56 and 64, respectively).



proportion of 3HHX monomer in P(3HB-co-3HHX) synthesized from *Cupriavidus necator* transformants [33]. *Enterobacter* sp. TS1L successfully synthesized mcl-co-lcl PHA containing 3HHD and 3HOD in a dual MFC system [34]. *Bacillus* sp. YHY22 could use lactate and propionate as substrates to produce P(3HB-co-3HV) in the harsh environment of high salinity [35]. *Halomonas alkaliantarctica* was able to convert crude glycerol into P(3HB-co-3HV) without the need for any precursor supplementation [36]. More importantly, the use of *Halomonas* for the production of P(3HB), P(3HB-co-3HHX), P(3HB-co-4HB), P(34HBHV), P(34HB), P(3HB-co-3HHX) and P(3HB) has been industrialized with a maximum annual production of 10,000 tons, and the use of *Cupriavidus necator* for the production of P(3HB-co-3HV) has been industrialized with a maximum annual production of 4000 tons [37]. These functional bacteria were also present in the WMFC systems of this study, with relatively high abundances, highlighting their critical roles in PHC biotransformation, bioelectricity generation and PHA biosynthesis. Compared to previous studies, this research uniquely highlighted the biphasic role and metabolic flexibility of dual-function bacteria, such as *Pseudomonas*, *Bacillus*, *Acinetobacter* and *Desulfosarcina*, in balancing bioelectricity generation and PHA biosynthesis. By analyzing the dynamic shifts in microbial community composition across eight-time nodes, this study provided a comprehensive understanding of how electroactive biofilms adapt to environmental changes, prioritizing electron transfer during early biofilm formation and carbon storage during stabilization. They contributed to electron transfer and bioelectricity generation during the early biofilm formation phase, while shifting toward PHA synthesis during the stabilization phase. Unlike earlier studies that focused on either bioelectricity generation or PHA production, this work demonstrated the dual functionality of key bacteria and their ability to switch between electrochemical activity and PHA biosynthesis based on substrate availability and biofilm maturity. This dynamic adaptation underscored the metabolic flexibility of the microbial communities in WMFCs, enabling efficient balancing of bioelectricity recovery and bioplastic production. The specific results and analyses were described in the following sections.

During the early stages of biofilm formation (days 0–20), the relative abundances of EAB, including *Desulfuromonas*, *Bacillus*, *Brevundimonas*, *Clostridium*, *Acidibacter*, *Geobacter*, *Flavobacterium*, *Shewanella*, *Acinetobacter*, *Desulfosarcina*, *Pseudomonas* and *Pelotomaculum*, increased significantly (Fig. 5). The rising trend in the abundance of EAB correlated with the rise in bioelectricity generation observed during this period (Fig. 2b). This clarified that the microbial community was primarily focused on establishing stable electroactive biofilms, with electron transfer and bioenergy production being the dominant metabolic activities. The stabilization of bioelectricity generation after day 20 (Fig. 2b) coincided with the stabilization of EAB populations, indicating that the microbial community had reached a steady state where electron transfer processes were optimized. The subsequent decline in bioelectricity after day 32 can be attributed to substrate consumption, which likely reduced the metabolic activity of EAB and limited the availability of electrons for transfer to the anode. This decline in bioelectricity generation was mirrored by the decreasing relative abundance of key EAB after day 32. The dual-functionality of certain bacteria, such as *Pseudomonas*, *Bacillus*, *Acinetobacter* and *Desulfosarcina*, was particularly noteworthy. These bacteria demonstrated both electrochemical activity and the ability to synthesize PHAs. During the initial phase (days 0–28), these bacteria primarily contributed to electron transfer and bioelectricity generation, as evidenced by the increase in their relative abundance and the corresponding rise in bioelectricity output. The involvement of these dual-function bacteria in bioelectricity generation during the early stage explained the relatively low PHA content observed during this period (Fig. 2c), as the metabolic focus was on electron transfer rather than carbon storage.

As the biofilm matured and stabilized (days 20–56), the focus of the microbial community shifted from bioelectricity generation to PHA biosynthesis. This shift was reflected in the changing relative

abundances of PHASB, including *Pseudomonas*, *Cupriavidus*, *Bacillus*, *Alcanivorax*, *Rhodococcus*, *Acinetobacter*, *Alcaligenes*, *Ochrobactrum*, *Halomonas*, *Enterobacter*, *Paracoccus*, *Thauera* and *Desulfosarcina*, which increased significantly during this period (Fig. 5). The rise in PHA-synthesizing bacteria corresponded with the rapid increase in PHA content observed from days 28–48 (Fig. 2c), indicating that the microbial community was diverting more carbon substrates toward intracellular PHA storage, rather than electron transfer. The functional shift of dual-function bacteria, including *Pseudomonas*, *Bacillus*, *Acinetobacter* and *Desulfosarcina*, from electrochemical activity to PHA biosynthesis was particularly significant. After day 28, as bioelectricity generation declined, these bacteria began to contribute more to PHA production, as evidenced by the alignment between their relative abundance and the trend in PHA content (Fig. 2c). This shift in metabolic function clarified that these bacteria were capable of adapting their metabolic pathways in response to environmental conditions, such as substrate availability and the energy demands of the biofilms. During the early phase, when electron transfer was prioritized, these bacteria used the available carbon for bioenergy production. However, as bioelectricity generation became less critical in the later phase, they became involved in intracellular PHA storage, achieving a functional shift from electrochemical activity to PHA biosynthesis. The biphasic role of these dual-function bacteria highlighted the metabolic flexibility of the microbial community in the WMFCs. This adaptability allowed the system to efficiently balance bioenergy production and carbon storage.

### 3.5. Network connection of functional microorganisms with bioelectricity, PHAs, TPHCs, VFAs and EPS during electroactive biofilm formation and stabilization in WMFCs

There was a strong correlation between the changes in the communities of *Pseudomonas*, *Cupriavidus*, *Bacillus*, *Alcanivorax*, *Rhodococcus*, *Acinetobacter*, *Alcaligenes*, *Ochrobactrum*, *Halomonas*, *Enterobacter*, *Paracoccus*, *Thauera* and *Desulfosarcina*, and the variables of voltage, current density and power density (Fig. 6). These bacteria contributed to the generation of bioelectricity by PHCs, and transferring the resulting electrons to the electrode through direct or mediated electron transfer mechanisms [20]. The strong correlation between these bacteria and bioelectricity generation indicated that their metabolic activities were closely aligned with the performance of WMFCs. During the early phase of biofilm formation, when bioelectricity generation was rapidly increasing (Fig. 2b), these bacteria played a dominant role in facilitating electron transfer, thereby driving the observed increases in voltage, current density and power density. The significant relationships among voltage, current density and power density further emphasized the interconnected nature of these variables (Fig. 2b), which were all direct indicators of the electrochemical performance of WMFCs. The coordinated increase in these parameters during the biofilm formation phase reflected the overall improvement in the system's capacity of bioenergy generation as the microbial communities matured and optimized their electron transfer processes.

The changes in the communities of *Desulfuromonas*, *Brevundimonas*, *Clostridium*, *Acidibacter*, *Geobacter*, *Flavobacterium*, *Shewanella* and *Pelotomaculum* were significantly correlated with PHA content, TPHC biodegradation ratio and VFA production (Fig. 6). This reflected that these bacteria were key players in TPHC bioconversion and the subsequent generation of VFAs, which served as precursors for PHA biosynthesis [6,10,17,30,31]. The significant relationship among PHA content, TPHC biodegradation and VFA production indicated the interdependence of these processes. As TPHC were degraded, the resulting VFAs provided the necessary carbon sources for PHA biosynthesis, leading to the observed enhancement in PHA content (Fig. 2c and 3). This relationship underscored the importance of efficient TPHC biodegradation and VFA production for maximizing PHA content, which was a key objective for bioresource recovery in WMFCs. In addition, the observed correlation between biofilm thickness and EPS peak height highlighted



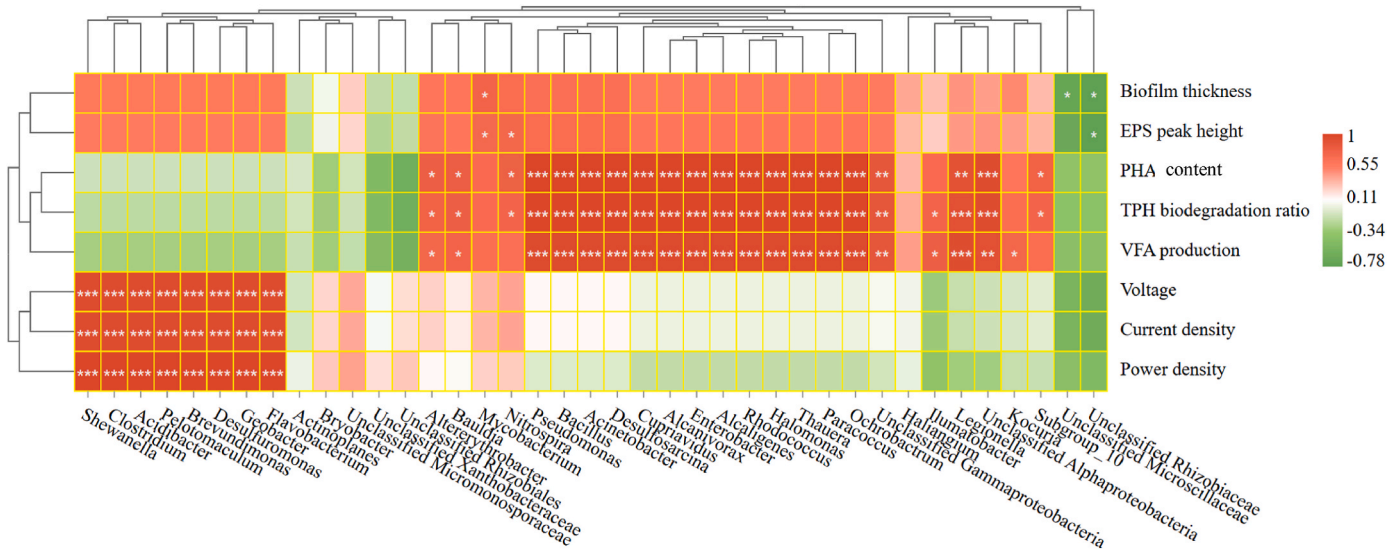


**Fig. 6.** Network connection of functional microorganisms with biofilm thickness, voltage, current density, power density, PHA content, VFA production, TPHC biodegradation ratio, EPS peak height during electroactive biofilm formation and stabilization in WMFCs.

that EPS, particularly tyrosine/tryptophan proteins, were key contributors to the structural integrity and functionality of electroactive biofilms (Fig. 2a and 4). EPS not only provided a scaffold for microbial attachment and biofilm cohesion but also enhanced bioconversion processes within the biofilms. This correlation reflected that the production and composition of EPS, especially proteins with redox-active amino acids like tyrosine and tryptophan, were critical for the development of robust and efficient electroactive biofilms, which in turn provided a stable microbial substrate and energetic support for the subsequent efficient synthesis of PHA.

4. Conclusions

This study offered novel insight into PHA production during electroactive biofilm formation and stabilization. The significant changes were observed in both current and power densities, which initially increased, remained stable in the middle stage and then decreased in the later stages. The produced PHAs were identified as P(3HB), P(3HV), P(3HB-co-3HV), P(3HB-co-3HHX), P(3HHD) and P(3HOD). The maximum PHA content was produced at 0.664 g g<sup>-1</sup> DCW. The trend of VFA production from days 0–56 exhibited a close correlation with TPHC biodegradation. A notable functional shift from bioelectricity generation to PHA biosynthesis was observed. The network connection of functional bacteria with bioelectricity, PHAs, TPHCs, VFAs and EPS was built. These findings enhance the understanding of electroactive biofilm dynamics and offer potential for sustainable PHA generation. Based on this study, future research could focus on exploring genetic modifications to further enhance electroactive biofilm performance and broaden its applications in clean bioresource synthesis.

CRediT authorship contribution statement

**Lanmei Zhao:** Writing – review & editing, Writing – original draft, Validation, Software, Resources, Methodology, Funding acquisition, Formal analysis, Data curation, Conceptualization. **Mengxue Sun:** Writing – original draft, Software, Data curation. **Can Lyu:** Supervision, Resources, Methodology, Funding acquisition. **Long Meng:** Supervision, Resources, Methodology, Funding acquisition. **Jian Liu:** Supervision, Resources, Methodology, Funding acquisition. **Bo Wang:** Supervision, Resources, Methodology, Funding acquisition.

Declaration of competing interest

The authors declare that they have no known competing financial interests or personal relationships that could have appeared to influence the work reported in this paper.

Acknowledgments

This study is supported by National Natural Science Foundation of China (42106144), Natural Science Foundation of Shandong Province (ZR2021QE125, ZR2020QD089 and ZR2023QC207), Science and Technology Project of Beijing Life Science Academy Company Limited (0002023CC0090), Natural Science Foundation of Qingdao City (23-2-1-52-zzyd-jch), and Central Public-interest Scientific Institution Basal Research Fund (1610232023020).

Appendix A. Supplementary data

Supplementary data to this article can be found online at <https://doi.org/10.1016/j.synbio.2025.01.008>.

References

[1] Wang B, Kuang S, Shao H, Cheng F, Wang H. Improving soil fertility by driving microbial community changes in saline soils of Yellow River Delta under petroleum pollution. *J Environ Manag* 2022;304:114265.

[2] Zhao X, Zhang Q, He G, Zhang L, Lu Y. Delineating pollution threat intensity from onshore industries to coastal wetlands in the bohai rim, the yangtze River Delta, and the pearl River Delta, China. *J Clean Prod* 2021;320:128880.

[3] Gebregiorgis Ambaye T, Vaccari M, Franzetti A, Prasad S, Formicola F, Rosatelli A, Hassani A, Aminabhavi TM, Rtimi S. Microbial electrochemical bioremediation of petroleum hydrocarbons (PHCs) pollution: recent advances and outlook. *Chem Eng J* 2023;452:139372.

[4] Zhao L, Zhao D. Hydrolyzed polyacrylamide biotransformation during the formation of anode biofilm in microbial fuel cell biosystem: bioelectricity, metabolites and functional microorganisms. *Bioresour Technol* 2022;360:127581.

[5] Kopperi H, Amulya K, Venkata Mohan S. Simultaneous biosynthesis of bacterial polyhydroxybutyrate (PHB) and extracellular polymeric substances (EPS): process optimization and Scale-up. *Bioresour Technol* 2021;341:125735.

[6] Idris S, Rahim RA, Amirul A-AA. Bioprospecting and molecular identification of used transformer oil-degrading bacteria for bioplastics production. *Microorganisms* 2022;10:1–12.

[7] Jeon J-M, Park S-J, Son Y-S, Yang Y-H, Yoon J-J. Bioconversion of mixed alkanes to polyhydroxyalkanoate by *Pseudomonas resinovorans*: upcycling of pyrolysis oil from waste-plastic. *Polymers* 2022;14:2624.

[8] Karthikeyan M, Aravindh A, Baskaran D, Murugappan R. Bioconversion of oily bilge waste to polyhydroxybutyrate (PHB) by marine *Ochrobactrum intermedium*. *Bioresour Technol Rep* 2018;4:66–73.

- [9] Mwamburi SM, Mbatia BN, Kasili R, Muge EK, Noah NM. Production of polyhydroxyalkanoates by hydrocarbon-aclastic bacteria. *Afr J Biotechnol* 2019;18: 352–64.
- [10] Sangkharak K, Choonut A, Rakkan T, Prasertsan P. The degradation of phenanthrene, pyrene, and fluoranthene and its conversion into medium-chain-length polyhydroxyalkanoate by novel polycyclic aromatic hydrocarbon-degrading bacteria. *Curr Microbiol* 2020;77:897–909.
- [11] Yajima T, Nagatomo M, Wakabayashi A, Sato M, Taguchi S, Maeda M. Bioconversion of biphenyl to a polyhydroxyalkanoate copolymer by *Alcaligenes denitrificans* A41. *Amb Express* 2020;10:155.
- [12] Rangel C, Lourenço ND, Reis MAM, Carvalho G. Dynamics in the profile of biopolymers produced by mixed microbial cultures from ethanol-rich feedstocks. *J Environ Chem Eng* 2024;12:112609.
- [13] Wen Q, Liu S, Lin X, Liu B, Chen Z. Rapid recovery of mixed culture polyhydroxyalkanoate production system from EPS bulking using azithromycin. *Bioresour Technol* 2022;350:126944.
- [14] Xi J, Fang W, Zhang H, Zhang J, Xu H, Zheng M. Promotion of polyhydroxyalkanoates-producing granular sludge formation by lactic acid using anaerobic dynamic feeding process. *J Biotechnol* 2024;395:84–94.
- [15] Zhao L, Bao M, Zhao D, Li F. Correlation between polyhydroxyalkanoates and extracellular polymeric substances in the activated sludge biosystems with different carbon to nitrogen ratio. *Biochem Eng J* 2021;176:108204.
- [16] Zhao L, Cheng Y, Yin Z, Chen D, Bao M, Lu J. Insights into the effect of different levels of crude oil on hydrolyzed polyacrylamide biotransformation in aerobic and anoxic biosystems: bioresource production, enzymatic activity, and microbial function. *Bioresour Technol* 2019;293:122023.
- [17] Zhao L, Liu J, Meng L, Zhao D, Wang B. Different dissolved oxygen levels drive polyhydroxyalkanoate biosynthesis from hydrolyzed polyacrylamide-containing oil sludge. *Process Saf Environ Protect* 2023;169:526–33.
- [18] Pi Y, Bao M, Liu Y, Lu T, He R. The contribution of chemical dispersants and biosurfactants on crude oil biodegradation by *Pseudomonas* sp. LSH-7<sup>+</sup>. *J Clean Prod* 2017;153(1):74–82.
- [19] Yu G-H, He P-J, Shao L-M, He P-P. Stratification structure of sludge flocs with implications to dewaterability. *Environ Sci Technol* 2008;42(21):7944–9.
- [20] Zhao L, Gao J, Meng L, Liu J, Zhao D. The effect of crude oil on hydrolyzed polyacrylamide-containing wastewater treatment using microbial fuel cell biosystem. *Process Saf Environ Protect* 2023;179:89–98.
- [21] Chen X, Han T, Miao X, Zhang X, Zhao L, Sun Y, Ye H, Li X, Li Y. Ferrihydrite enhanced the electrogenic hydrocarbon degradation in soil microbial electrochemical remediation. *Chem Eng J* 2022;446:136901.
- [22] Wang H, Cui Y, Lu L, Jin S, Zuo Y, Ge Z, Ren ZJ. Moisture retention extended enhanced bioelectrochemical remediation of unsaturated soil. *Sci Total Environ* 2020;724:138169.
- [23] Zhang X, Li X, Zhao X, Chen X, Zhou B, Weng L, Li Y. Bioelectric field accelerates the conversion of carbon and nitrogen in soil bioelectrochemical systems. *J Hazard Mater* 2020;388:121790.
- [24] Liang Y, Zhai H, Liu B, Ji M, Li J. Carbon nanomaterial-modified graphite felt as an anode enhanced the power production and polycyclic aromatic hydrocarbon removal in sediment microbial fuel cells. *Sci Total Environ* 2020;713:136483.
- [25] Zhao L, Deng J, Hou H, Li J, Yang Y. Investigation of PAH and oil degradation along with electricity generation in soil using an enhanced plant-microbial fuel cell. *J Clean Prod* 2019;221:678–83.
- [26] Yu L, He D, Zhang E, He Q, Li J, Ren ZJ, Zhou S. Electricity from anaerobic methane oxidation by a single methanogenic archaeon *Methanosarcina barkeri*. *Chem Eng J* 2021;405:126691.
- [27] Zhang X, Li R, Song J, Ren Y, Luo X, Li Y, Li X, Li T, Wang X, Zhou Q. Combined phyto-microbial-electrochemical system enhanced the removal of petroleum hydrocarbons from soil: a profundity remediation strategy. *J Hazard Mater* 2021; 420:126592.
- [28] Zhao F, Heidrich ES, Curtis TP, Dolfing J. The effect of anode potential on current production from complex substrates in bioelectrochemical systems: a case study with glucose. *Appl Microbiol Biotechnol* 2020;104:5133–43.
- [29] Srikanth S, Reddy MV, Mohan SV. Microaerophilic microenvironment at biocathode enhances electrogenesis with simultaneous synthesis of polyhydroxyalkanoates (PHA) in bioelectrochemical system (BES). *Bioresour Technol* 2012;125:291–9.
- [30] Corti Monzon G, Bertola G, Herrera Seitz MK, Murialdo SE. Exploring polyhydroxyalkanoates biosynthesis using hydrocarbons as carbon source: a comprehensive review. *Biodegradation* 2024;35:519–38.
- [31] Crisafi F, Valentino F, Micolucci F, Denaro R. From organic wastes and hydrocarbons pollutants to polyhydroxyalkanoates: bioconversion by terrestrial and marine bacteria. *Sustainability* 2022;14:8241.
- [32] Bellary S, Patil M, Mahesh A, Lali A. Microbial conversion of lignin rich biomass hydrolysates to medium chain length polyhydroxyalkanoates (mcl-PHA) using *Pseudomonas putida* KT2440. *Prep Biochem Biotechnol* 2023;53:54–63.
- [33] Tan HT, Chek MF, Lakshmanan M, Foong CP, Hakoshima T, Sudesh K. Evaluation of BP-M-CPF4 polyhydroxyalkanoate (PHA) synthase on the production of poly(3-hydroxybutyrate-co-3-hydroxyhexanoate) from plant oil using *Cupriavidus necator* transformants. *Int J Biol Macromol* 2020;159:250–7.
- [34] Chaijak P, Rakkan T, Paichaid N, Thipraksa J, Michu P, Sangkharak K. Exploring potential Aspect of microbial fuel cell (MFC) for simultaneous energy, polyhydroxyalkanoate (PHA) production and textile wastewater (TW) treatment. *J Polym Environ* 2024;32:3104–18.
- [35] Lee HJ, Kim SG, Cho DH, Bhatia SK, Gurav R, Yang SY, Yang J, Jeon JM, Yoon JJ, Choi KY, Yang YH. Finding of novel lactate utilizing *Bacillus* sp. YHY22 and its evaluation for polyhydroxybutyrate (PHB) production. *Int J Biol Macromol* 2022; 201:653–61.
- [36] Mozejko-Ciesielska J, Moraczewski K, Czaplicki S. *Halomonas alkaliantartica* as a platform for poly(3-hydroxybutyrate-co-3-hydroxyvalerate) production from biodiesel-derived glycerol. *Environ. Microbiol. Rep.* 2024;16(1):e13225.
- [37] Diankrstanti PA, Lin YC, Yi YC, Ng IS. Polyhydroxyalkanoates bioproduction from bench to industry: thirty years of development towards sustainability. *Bioresour Technol* 2024;393:130149.